

Distorted Wave Calculations of (d,p) Angular Distributions*

WILLIAM R. SMITH† AND EUGENE V. IVASH
The University of Texas, Austin, Texas
 (Received June 18, 1962)

Deuteron stripping differential cross sections based on the distorted wave Born approximation with diffuse-well nuclear optical potentials have been calculated for a large number of reactions, using mainly a program whose average running time on a CDC 1604 computer is about 3 sec. In general, good agreement between theoretical and experimental results has been obtained for nuclei with $A \geq 59$ using nuclear parameters which are relatively constant. It has been found that best-fit elastic scattering optical parameters give good results for nuclei in this region. The effect of spin-orbit interactions on differential cross sections and on polarizations has also been examined.

INTRODUCTION

ELASTIC nuclear scattering of particles of various kinds has been studied extensively using the optical model.¹ The optimum nuclear parameters obtained have been found to vary slowly and systematically as a function of the bombarding energy and target weight.²

For stripping reactions the simple direct interaction theory of Butler³ has provided semiquantitative agreement with a large body of data. Its use, in principle, is restricted to energies high enough that Coulomb and nuclear distortion effects can be approximately neglected.

The calculations presented here⁴ for (d,p) reactions are based on the distorted wave Born approximation.^{5,6} Tapered-well optical potentials similar to the Woods-Saxon potential are used (see Fig. 1), radial integrals are extended to the origin, and Coulomb effects are taken into account. The stripping amplitude has the form of a sum of radial integrals, with each integrand involving the combined product of deuteron, proton, and neutron radial wave functions, each function being the solution with appropriate boundary conditions and parameters of the radial Schrödinger equation

$$\psi''(r) - \frac{2\mu}{\hbar^2} \left[E + VF_R + iWF_I + V_c - \frac{\hbar^2 L(L+1)}{2\mu r^2} \right] \psi(r) = 0.$$

Here V and W are, respectively, the real and imaginary potential depths, F_R and F_I are the optical well form factors as defined in Fig. 1, L is the orbital quantum number, and V_c is the appropriate Coulomb interaction potential.

* This work was supported in part by the U. S. Atomic Energy Commission and the Air Force Office of Scientific Research.

† Submitted in partial fulfillment of the requirements for the Ph.D. degree at the University of Texas.

¹ H. Feshbach, C. E. Porter, and V. F. Weisskopf, *Phys. Rev.* **96**, 448 (1954).

² F. Bjorklund, G. Campbell, and S. Fernbach, *International Symposium on Polarization Phenomena of Nucleons*, Basel, 1960 [*Helv. Phys. Acta.*, Suppl. 6, (1961)], p. 432.

³ S. T. Butler, *Proc. Roy. Soc. (London)* **A208**, 559 (1951).

⁴ The calculations were performed on the CDC 1604 computer at the University of Texas.

⁵ W. Tobocman, *Phys. Rev.* **94**, 1655 (1954).

⁶ R. Huby, M. Y. Refai, and G. R. Satchler, *Nuclear Phys.* **9** 94 (1958).

It was found that equating the neutron potential form factor to the real part of the deuteron form factor gave somewhat better results than the apparently more plausible procedure of setting it equal to the real part of the proton form factor. Consequently, in the calculations presented here, the neutron and real deuteron form factors are taken to be identical.

If the optical potential model is valid for stripping, it is expected, as is the case for elastic scattering,² that there exists a slowly-varying set of optical parameters capable of explaining a wide range of nuclear processes. In addition, the parameters obtained from stripping calculations should agree with the corresponding parameters for elastic scattering. We have examined both stripping and elastic scattering angular distributions in order to determine the extent to which the above expectations can be fulfilled.

CALCULATIONAL PROCEDURE

Our investigations have shown that the effect of varying the optical parameters for stripping is, in general, much the same as it is for elastic scattering. In addition, variation of the deuteron parameters results in approximately the same behavior of the angular distribution as variation of the proton parameters. However, an effect that is present for a certain

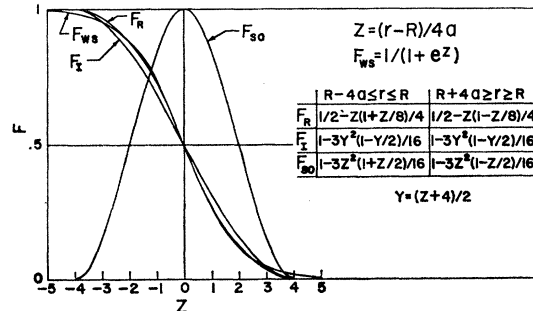


FIG. 1. Comparison of the real (F_R) and imaginary (F_I) potential form factors, used in this work, with the Woods-Saxon (F_{WS}) form factor. The difference in results between using these wells and using the Woods-Saxon well is small. Woods-Saxon wells have been used in the elastic scattering calculations. The spin-orbit form factor is given by the expression $0.511F_{SO}/ra$ and has the same value at the radius R as the usual derivative form factor.

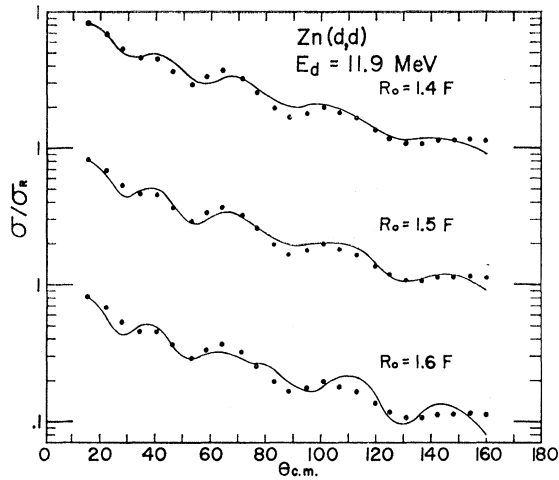


FIG. 2. Comparison of experimental and theoretical angular distributions for the elastic scattering of 11.8-MeV deuterons on Zn. This figure provides a visual estimate of the degree of fit indicated by root-mean-square deviation, parameter Δ , as given in Table III.

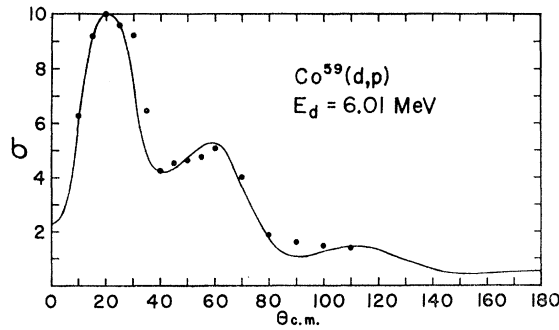


FIG. 3. Comparison of experimental and theoretical angular distributions for the $Co^{59}(d,p)Co^{60}$ ground-state reaction, $E_d=6.01$ MeV, $L_N=1$, $Q=5.262$ MeV. The parameters are listed in Table II.

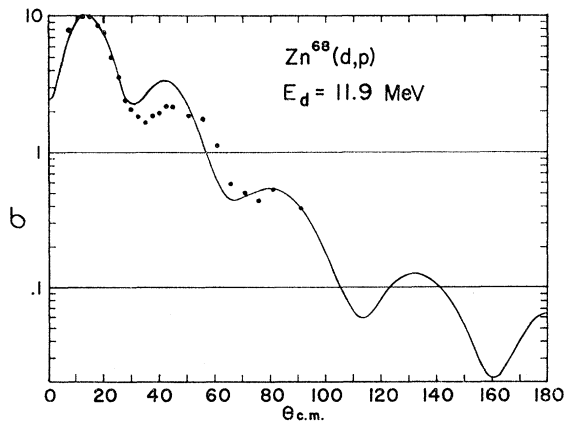


FIG. 4. Comparison of experimental and theoretical angular distributions for the $Zn^{68}(d,p)Zn^{69}$ ground-state reaction, $E_d=11.9$ MeV, $L_N=1$, $Q=4.266$ MeV. The parameters are listed in Table II.

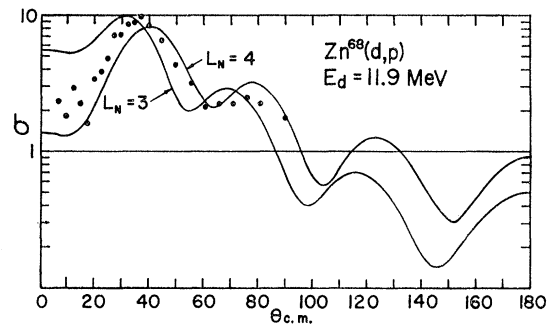


FIG. 5. Comparison of experimental and theoretical angular distributions for the $Zn^{68}(d,p)Zn^{69}$ 0.44-MeV level reaction, $E_d=11.9$ MeV, $L_N=3, 4$, $Q=3.826$ MeV. The parameters are listed in Table II.

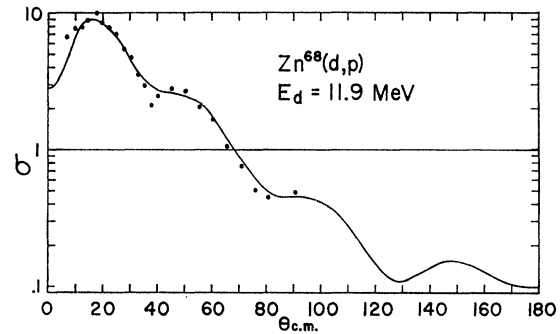


FIG. 6. Comparison of experimental and theoretical angular distributions for the $Zn^{68}(d,p)Zn^{69}$ 0.82-MeV level reaction, $E_d=11.9$ MeV, $Q=3.446$ MeV. The curve is the sum of cross sections, obtained using $2p_{1/2}$ and $2d_{3/2}$ neutron orbitals, added in the ratio of their calculated absolute cross sections, it being assumed that the spins of the levels involved have the maximum values allowed. The parameters are listed in Table II.

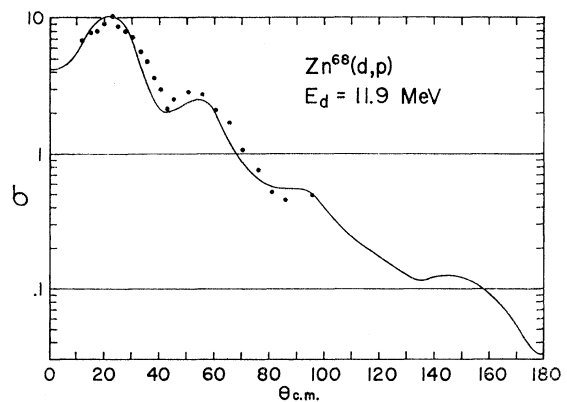


FIG. 7. Comparison of experimental and theoretical angular distributions for the $Zn^{68}(d,p)Zn^{69}$ 0.82-MeV level reaction, $E_d=11.9$ MeV, $Q=3.446$ MeV. A $1d$ neutron orbital is used. The parameters are listed in Table II.

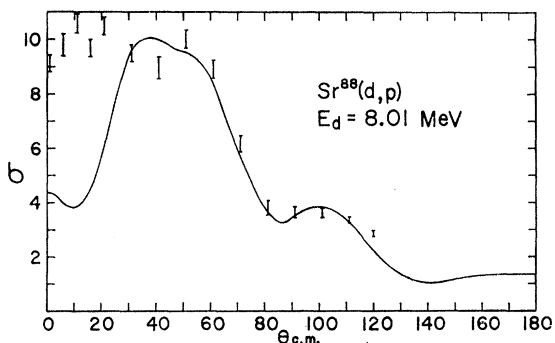


FIG. 8. Comparison of experimental and theoretical angular distributions for the $\text{Sr}^{88}(d,p)\text{Sr}^{89}$ ground-state reaction, $E_d=8.01$ MeV, $L_N=2$, $Q=3.11$ MeV. The parameters are listed in Table II.

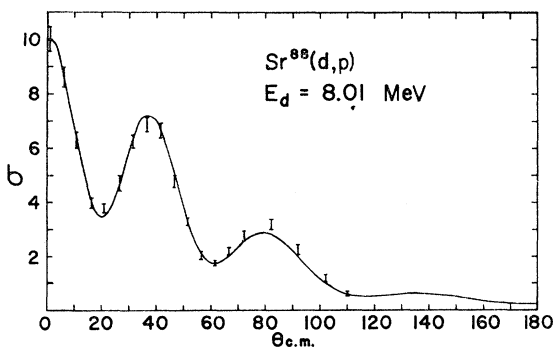


FIG. 9. Comparison of experimental and theoretical angular distributions for the $\text{Sr}^{88}(d,p)\text{Sr}^{89*1.07}$ -MeV level reaction, $E_d=8.01$ MeV, $L_N=0$, $Q=4.18$ MeV. The parameters are listed in Table II.

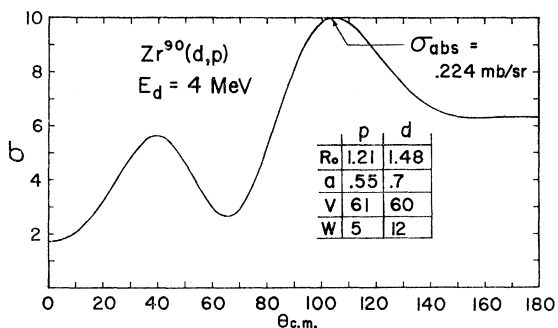


FIG. 10. Theoretical angular distribution for the $\text{Zr}^{90}(d,p)\text{Zr}^{91*1.22}$ -MeV level reaction, $E_d=4$ MeV, $L_N=0$, $Q=3.8$ MeV.

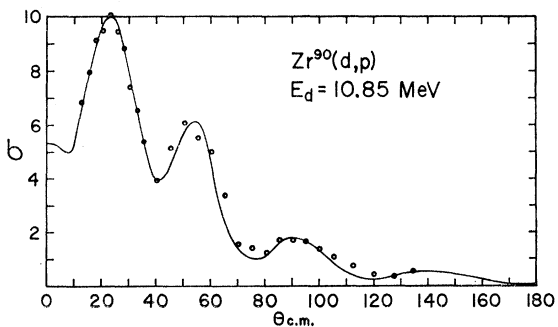


FIG. 11. Comparison of experimental and theoretical angular distributions for the $\text{Zr}^{90}(d,p)\text{Zr}^{91}$ ground-state reaction, $E_d=10.85$ MeV, $L_N=2$, $Q=5.02$ MeV. The parameters are listed in Table II.

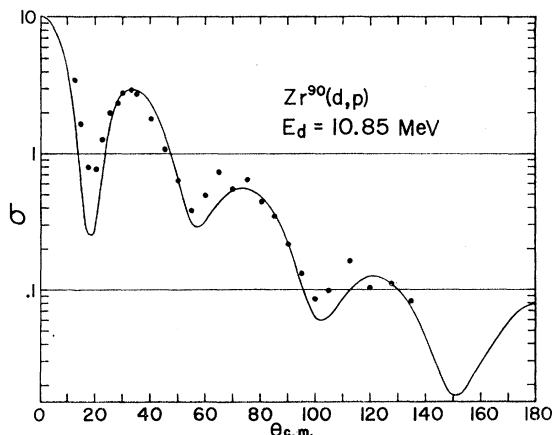


FIG. 12. Comparison of experimental and theoretical angular distributions for the $\text{Zr}^{90}(d,p)\text{Zr}^{91*1.22}$ -MeV level reaction, $E_d=10.85$ MeV, $L_N=0$, $Q=3.8$ MeV. The parameters are listed in Table II.

range of parameter variation for one of the particles often persists over a considerably greater range of variation of the parameters for the other particle.

In most cases studied here, increasing either V or R for the proton or deuteron causes the diffraction maxima in the angular distribution to move from large angles toward small angles, appearing on the right and disappearing on the left as these parameters are increased. The rate at which a given maximum travels is approximately proportional to its angular position. Increasing W for either proton or deuteron smooths out the maxima and minima. Provided the cross section is plotted on a logarithmic scale and normalized at some fixed angle, increasing the diffusion parameter a rotates the distribution clockwise about the normalization point. The effect of varying the neutron parameters may be markedly different for various reactions, but, in general, the positions of the maxima and minima tend to remain unchanged. The effect of modifying the proton or deuteron absorption from a volume to a surface type of interaction also was investigated. It was observed that the central region of the angular distribution is raised as the surface interaction is made dominant. The inclusion of spin-orbit interactions, at least for the case that the total angular momentum quantum number of the neutron is $\frac{1}{2}$, was found, as expected, to depress the maxima, raise the minima, and in many cases to slightly shift the distribution toward smaller angles.

The $\text{Sr}^{88}(d,p)\text{Sr}^{89*1.07}$ -MeV level reaction was the first to be considered for a heavier nucleus. It was found that the observed angular distribution could be fitted using parameters which agreed approximately with those for elastic scattering. The calculations were then extended to other reactions for medium and heavy nuclei, attempting to keep the variation in the parameters from one nucleus to the next as systematic as possible. The results of this procedure are shown in

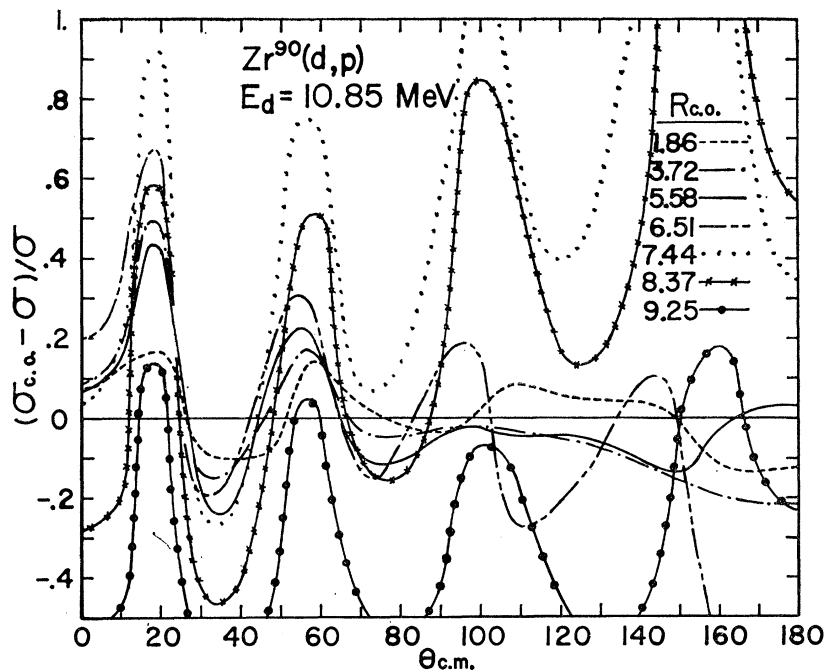


FIG. 13. Same case as Fig. 12, except that the interior radial integration is cut off at the radii indicated.

Figs. 3-20, while Table I lists the general properties of the stripping reactions studied, and Table II presents the relevant parameters. The cross sections are relative, being normalized at the main stripping peak if this is well defined; otherwise, the normalization is such as to give the best over-all agreement between calculation and experiment.

Best-fit (in the least-squares sense⁷) non-spin-orbit elastic scattering parameters were also utilized in order to investigate their applicability to stripping. The angular distributions so obtained are presented in Figs. 21-29, with Table III listing the parameters used for the various reactions. No suitable elastic scattering proton data were available for the $Ce^{140}(d,p)Ce^{141}$

TABLE I. List of stripping reactions.

Target nucleus	Residual level	Level energy (MeV)	E_d (MeV)	Q (MeV)	Neutron orbital	Figure	Reference
Co^{69}	0	0	6.01	5.262	$2p_{3/2}$	3, 21	b
Zn^{68}	0	0	11.9	4.266	$2p_{1/2}$	4, 22, 23	c
	1	0.44		3.826	a	5	
	2	0.82		3.446	a	6, 7	
Sr^{88}	0	0	8.01	4.18	$2d_{5/2}$	8	d
	1	1.07		3.11	$3s_{1/2}$	9	
	0	0		5.02	$2d_{5/2}$	11	
Zr^{90}	0	0	10.85	5.02	$2d_{5/2}$	12	e
	1	1.22		3.80	$3s_{1/2}$	16	
	0	0		13.6	5.02	$2d_{5/2}$	
Zr^{90}	1	1.22	13.6	3.80	$3s_{1/2}$	16	f
	0	0		4.85	$3s_{1/2}$	17, 26	
	1	0.16		4.69	$2d_{3/2}$	18, 27	
Ce^{140}	0	0	10.85	3.21	$2f_{7/2}$	19	h
	1	0.65		2.56	$3p_{3/2}$	20	
	0	0		10.85	4.51	$3p_{1/2}$	
Pb^{206}	0	0	10.85	4.51	$3p_{1/2}$	28	i
Pb^{208}	3	2.	15.	-0.29	$4s_{1/2}$	29	j

* Orbitals are given in the figure captions.

^b H. A. Enge, D. L. Jarrell, and C. C. Angleman, Phys. Rev. **119**, 735 (1960).

^c F. S. Eby, Phys. Rev. **96**, 1355 (1954).

^d J. R. Holt and T. N. Marsham, Proc. Phys. Soc. (London) **A66**, 565 (1953).

^e R. L. Preston, H. J. Martin, and M. B. Sampson, Phys. Rev. **121**, 1741 (1961).

^f N. I. Zaika and O. F. Nemets, J. Exptl. Theoret. Phys. U.S.S.R. **40**, 1019 (1961) [translation: Soviet Phys.—JETP **13**, 716 (1961)].

^g B. L. Cohen and R. E. Price, Phys. Rev. **121**, 1441 (1961).

^h G. B. Holm and H. J. Martin, Phys. Rev. **122**, 1537 (1961).

ⁱ M. T. McEllistrem, H. J. Martin, D. W. Miller, and M. B. Sampson, Phys. Rev. **111**, 1636 (1958).

^j B. L. Cohen, R. E. Price, and S. Mayo, Nuclear Phys. **20**, 370 (1960).

⁷ A. E. Glassgold and P. J. Kellogg, Phys. Rev. **107**, 1372 (1957).

TABLE II. Stripping parameters.

Target nucleus	Residual level	E_d (MeV)	Deuteron or proton	R_0 (F)	a (F)	V (MeV)	W (MeV)	σ_{th}/σ_{exp}	Figure
Co ⁶⁹	0	6.01	d	1.50	0.70	60	16	2.28	3
			p	1.22	0.55	53	8		
Zn ⁶⁸	0	11.9	d	1.48	0.65	60	16		4
			p	1.21	0.55	57	8		
Zn ⁶⁸	1	11.9	d	1.48	0.65	60	16		5
			p	1.21	0.55	57	8		
Zn ⁶⁸	2	11.9	d	1.48	0.65	60	16		6, 7
			p	1.21	0.55	57	8		
Sr ⁸⁸	0	8.01	d	1.48	0.68	60	16		8
			p	1.21	0.53	59.5	8.5		
Sr ⁸⁸	1	8.01	d	1.48	0.68	60	16		9
			p	1.21	0.53	59.5	8.5		
Zr ⁹⁰	0	10.85	d	1.48	0.70	60	16	2.92	11
			p	1.21	0.55	57	8		
Zr ⁹⁰	1	10.85	d	1.48	0.70	60	16	2.88	12
			p	1.21	0.55	57	8		
Zr ⁹⁰	0	13.6	d	1.48	0.70	65	18		15
			p	1.21	0.55	56	8		
Zr ⁹⁰	1	13.6	d	1.48	0.70	65	20		16
			p	1.21	0.55	56	10		
Sn ¹¹⁶	0	15.0	d	1.48	0.70	58	16	2.02	17
			p	1.21	0.55	52	8		
Sn ¹¹⁶	1	15.0	d	1.48	0.70	58	12	1.89	18
			p	1.21	0.55	52	5.5		
Ce ¹⁴⁰	0	10.85	d	1.48	0.75	48	12	2.58	19
			p	1.16	0.60	60	10		
Ce ¹⁴⁰	1	10.85	d	1.48	0.75	48	12	1.67	20
			p	1.16	0.60	60	10		

reaction; however, optimum deuteron elastic scattering parameters were obtained, and these are shown together with the stripping deuteron parameters found independently. Identical elastic scattering parameters are used for the $Pb^{206}(d, p)Pb^{207}$ and $Pb^{208}(d, p)Pb^{209}$ reactions. Since the same nuclear parameters are used for all levels of a given nucleus, only the ground levels are listed in Table III.

RESULTS FOR ELEMENTS WITH $A \geq 59$

The angular distributions presented in Figs. 3-29 have, with the exception of Co⁶⁹, Sr⁸⁸, Ce¹⁴⁰, and Pb²⁰⁶

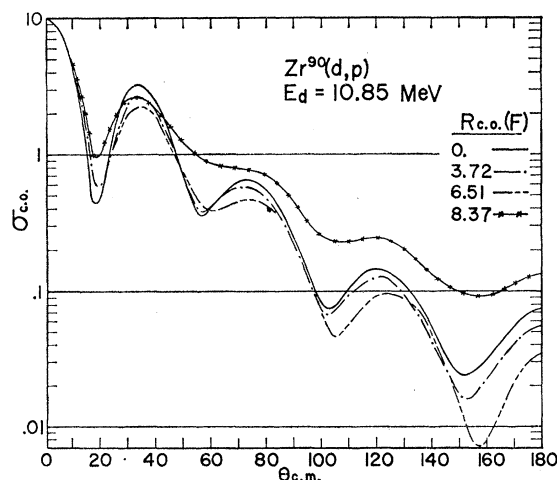


FIG. 14. Another representation of some of the cross sections in Fig. 13. The curves are normalized at 0°.

target nuclei reactions, been calculated for deuteron bombarding energies above the Coulomb barrier. Values of the orbital angular momentum quantum number L_N of the captured neutron range from 0 to 4. Because of the lack of additional data, results are only presented for a single bombarding energy with the exception of the Zr⁹⁰ reactions for which experimental angular distributions at two energies are available. An attempt was made to keep the nuclear parameters the same, or nearly so, for reactions leading to different states of the same residual nucleus.

In the initial study of stripping on targets with $A \geq 59$ little attention was paid to elastic scattering parameters because earlier results for lighter elements proved to be discouraging. Therefore, trial-and-error methods in fitting the angular distributions were at first used (Figs. 3-20 and Table II).

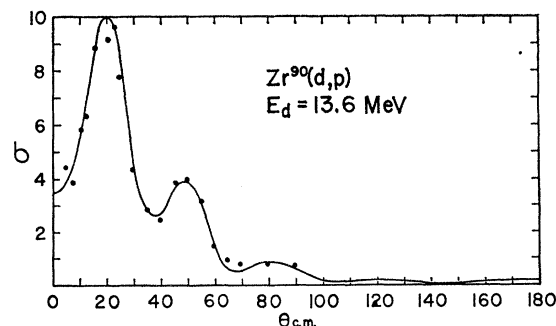


FIG. 15. Comparison of experimental and theoretical angular distributions for the $Zr^{90}(d, p)Zr^{91}$ ground-state reaction, $E_d = 13.6$ MeV, $L_N = 2$, $Q = 5.02$ MeV. The parameters are listed in Table II.

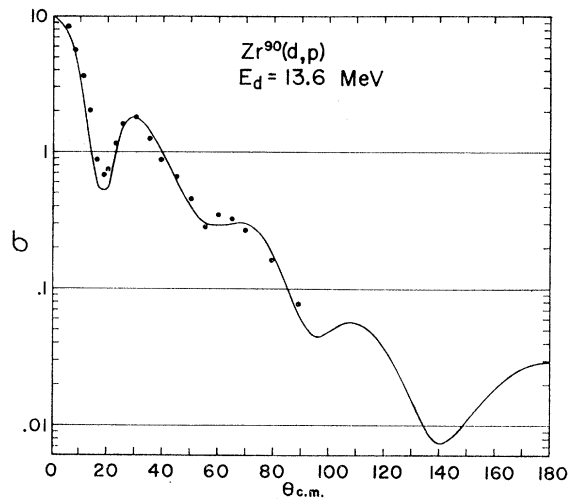


FIG. 16. Comparison of experimental and theoretical angular distributions for the $Zr^{90}(d,p)Zr^{91*1.22}$ -MeV level reaction, $E_d=13.6$ MeV, $L_N=0$, $Q=3.8$ MeV. The parameters are listed in Table II.

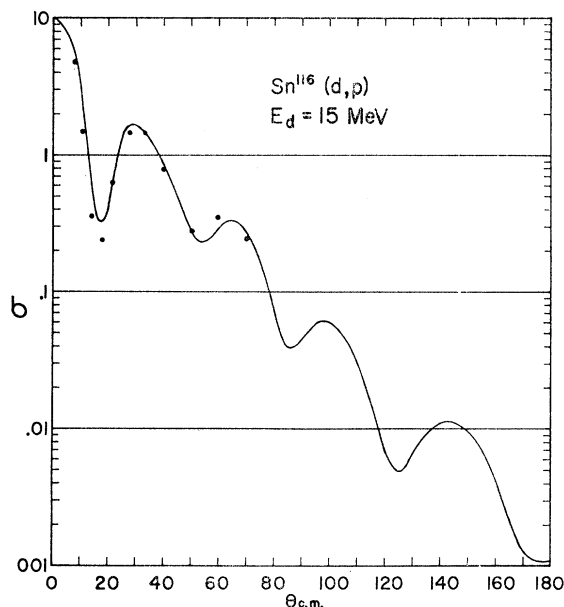


FIG. 17. Comparison of experimental and theoretical angular distributions for the $Sn^{116}(d,p)Sn^{117}$ ground-state reaction, $E_d=15$ MeV, $L_N=0$, $Q=4.85$ MeV. The parameters are listed in Table II.

The elements in the region $A=70-90$ seemed to require somewhat larger real potentials for the proton or deuteron than did the lighter element Co^{59} and the heavier elements Sn^{116} and Ce^{140} . It was also found for the first two cases that varying the proton potential in a suitable manner could compensate approximately for limited changes in the deuteron potential, and vice versa. The results of Melkanoff⁸ for deuteron elastic

⁸ M. A. Melkanoff, *Proceedings of the International Conference on the Nuclear Optical Model, Florida State University Studies, No. 32* (Rose Printing Company, Tallahassee, Florida, 1959), p. 207.

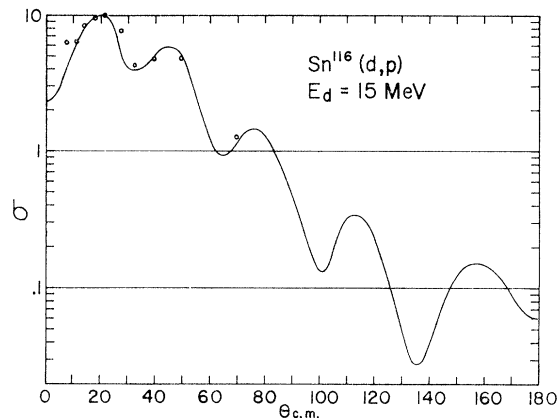


FIG. 18. Comparison of experimental and theoretical angular distributions for the $Sn^{116}(d,p)Sn^{117*0.16}$ -MeV level reaction, $E_d=15$ MeV, $L_N=2$, $Q=4.69$ MeV. The parameters are listed in Table II.

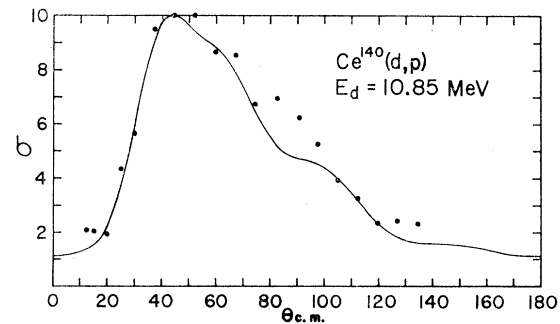


FIG. 19. Comparison of experimental and theoretical angular distributions for the $Ce^{140}(d,p)Ce^{141}$ ground-state reaction, $E_d=10.85$ MeV, $L_N=3$, $Q=3.21$ MeV. The parameters are listed in Table II.

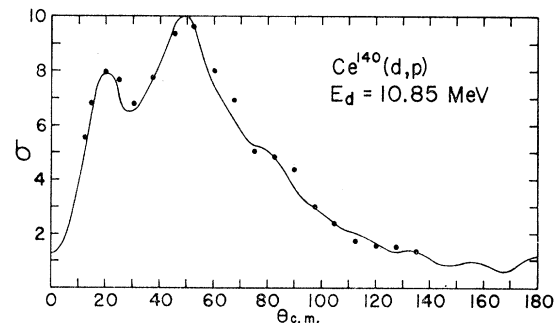


FIG. 20. Comparison of experimental and theoretical angular distributions for the $Ce^{140}(d,p)Ce^{141*0.65}$ -MeV level reaction, $E_d=10.85$ MeV, $L_N=1$, $Q=2.56$ MeV. The parameters are listed in Table II.

scattering agree with ours in that he finds the product VR^2 to be maximum in the region $A \approx 100$.

In subsequent studies appropriate elastic scattering parameters were obtained either from published results, when existent, or from our own work when not. These were then used for preliminary stripping calculations. Typical results for deuteron elastic scattering are pre-

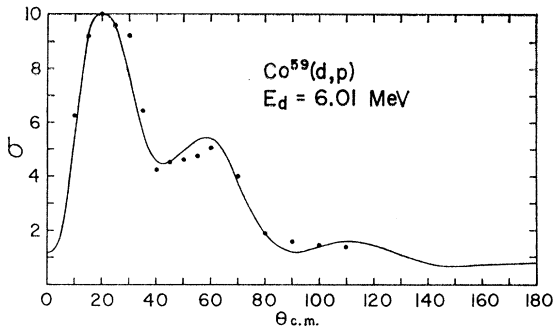


FIG. 21. Comparison of experimental and theoretical angular distributions for the $\text{Co}^{59}(d, p)\text{Co}^{60}$ ground-state reaction, $E_d = 6.01$ MeV, $L_N = 1$, $Q = 5.262$ MeV. The parameters used are similar to elastic scattering parameters and are listed in Table III.

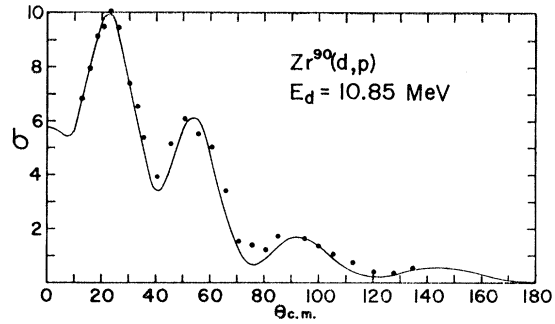


FIG. 24. Comparison of experimental and theoretical angular distributions for the $\text{Zr}^{90}(d, p)\text{Zr}^{91}$ ground-state reaction, $E_d = 10.85$ MeV, $L_N = 2$, $Q = 5.02$ MeV. The parameters used are similar to elastic scattering parameters and are listed in Table III.

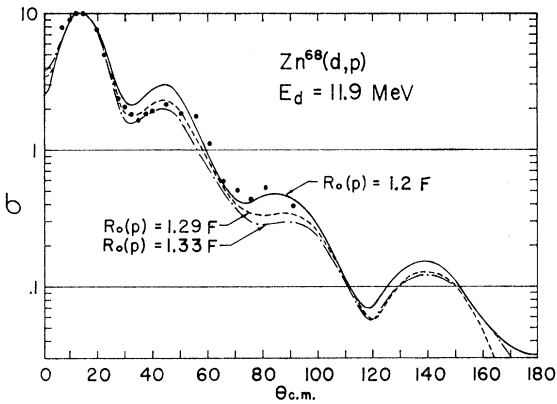


FIG. 22. Comparison of experimental and theoretical angular distributions for the $\text{Zn}^{68}(d, p)\text{Zn}^{69}$ ground-state reaction, $E_d = 11.9$ MeV, $L_N = 1$, $Q = 4.266$ MeV. The separate curves correspond to calculations for different proton potential radii. The parameters used are best-fit elastic scattering parameters and are listed in Table III.

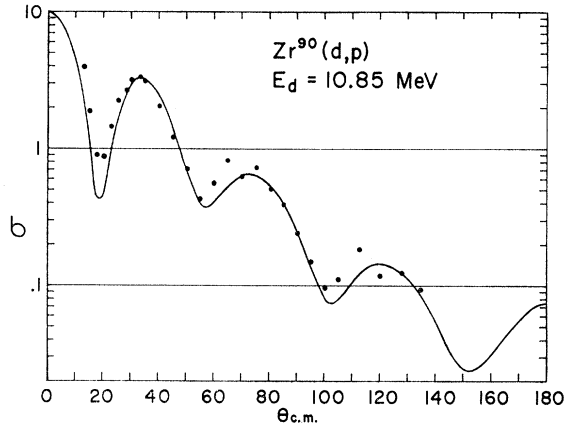


FIG. 25. Comparison of experimental and theoretical angular distributions for the $\text{Zr}^{90}(d, p)\text{Zr}^{91}$ 1.22-MeV level reaction, $E_d = 10.85$ MeV, $L_N = 0$, $Q = 3.8$ MeV. The parameters used are similar to elastic scattering parameters and are listed in Table III.

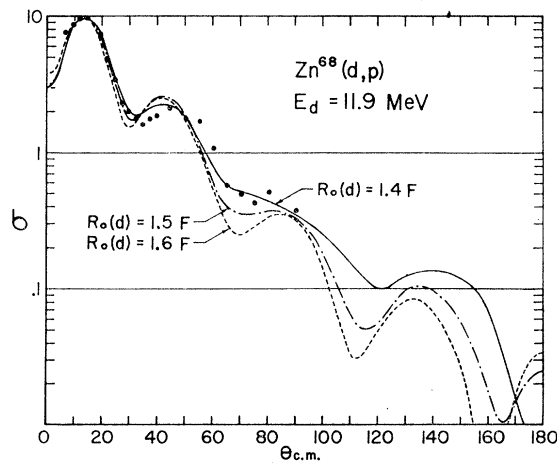


FIG. 23. Comparison of experimental and theoretical angular distributions for the $\text{Zn}^{68}(d, p)\text{Zn}^{69}$ ground-state reaction, $E_d = 11.9$ MeV, $L_N = 1$, $Q = 4.266$ MeV. The separate curves correspond to calculations for different deuteron potential radii. The parameters used are best-fit elastic scattering parameters and are listed in Table III.

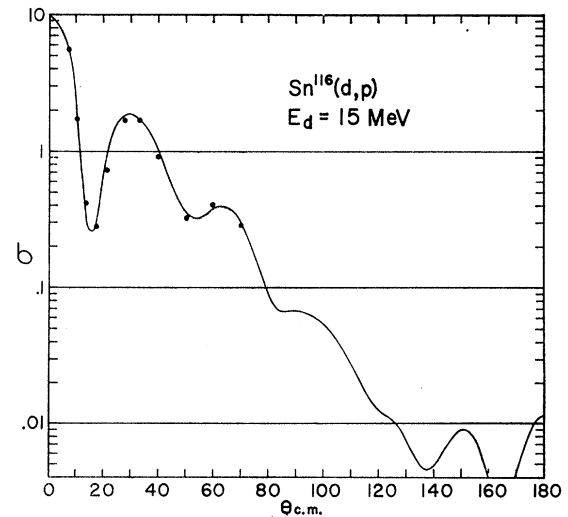


FIG. 26. Comparison of experimental and theoretical angular distributions for the $\text{Sn}^{116}(d, p)\text{Sn}^{117}$ ground-state reaction, $E_d = 15$ MeV, $L_N = 0$, $Q = 4.85$ MeV. The parameters used are similar to elastic scattering parameters and are listed in Table III.

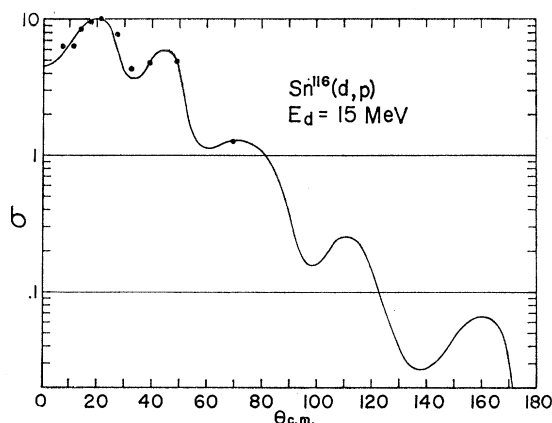


FIG. 27. Comparison of experimental and theoretical angular distributions for the $\text{Sn}^{116}(d,p)\text{Sn}^{117*0.16}$ -MeV level reaction, $E_d=15$ MeV, $L_N=2$, $Q=4.69$ MeV. The parameters used are similar to elastic scattering parameters and are listed in Table III.

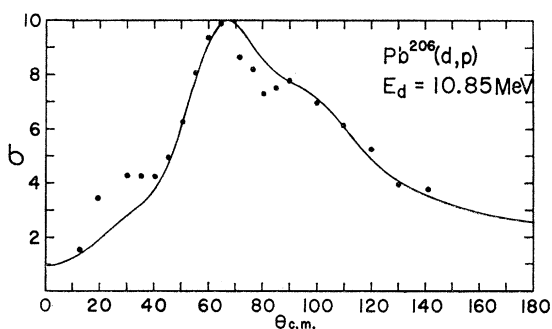


FIG. 28. Comparison of experimental and theoretical angular distributions for the $\text{Pb}^{206}(d,p)\text{Pb}^{207}$ ground-state reaction, $E_d=10.85$ MeV, $L_N=1$, $Q=4.51$ MeV. The parameters used are similar to elastic scattering parameters and are listed in Table III.

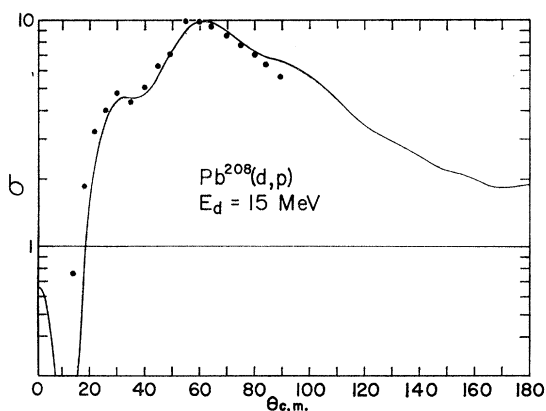


FIG. 29. Comparison of experimental and theoretical angular distributions for the $\text{Pb}^{208}(d,p)\text{Pb}^{209*2.0}$ -MeV level reaction, $E_d=15$ MeV, $L_N=0$, $Q=-0.29$ MeV. The parameters used are similar to elastic scattering parameters and are listed in Table III.

sented in Fig. 2 for Zn. In all cases attempted it was found that a set of parameters differing only slightly from the initial parameters, if at all, resulted in satisfactory agreement with the stripping data (Figs. 21-29 and Table III).

In all cases, the agreement between the calculated and observed angular distributions ranges from fair to excellent. For the Co^{59} , Sr^{88} , Zr^{90} , and Ce^{140} reactions shown in Figs. 3, 8, 11, and 20, respectively, the agreement is remarkably good, even at backward scattering angles.

For the $\text{Zn}^{68}(d,p)\text{Zn}^{69*0.44}$ -MeV level reaction calculations have been made on the basis of a $1g$ assignment for the captured state (expected on the basis of the shell model), as well as for a $1f$ orbital. The results in Fig. 5 slightly favor the former choice. The values of the nuclear parameters for this reaction have not been optimized as for most of the other cases considered, but are those determined for the ground-state transition. This is because a separate computer program with a comparatively much longer running time was used for cases in which the neutron is captured with an orbital angular momentum larger than two, and only a limited number of calculations were considered to be practicable. A similar situation exists for the $\text{Ce}^{140}(d,p)\text{Ce}^{141}$ ground-state reaction (Fig. 19). A $2f$ orbital was here assumed, and optical parameters were taken from the 0.65-MeV level calculation.

For the $\text{Zn}^{68}(d,p)\text{Zn}^{69*0.82}$ -MeV level reaction for which the experimental resolution is poor, a combination of cross sections corresponding to $2p_{3/2}$ and $2d_{5/2}$ orbitals has been calculated, and the two angular distributions added in the ratio of their absolute cross sections. A good fit is obtained (Fig. 6). Alternatively, following a suggestion of Raz,⁹ a $1d$ orbital has been tried, and also found to give a good fit (Fig. 7).

Difficulties were encountered with the reaction leading to the ground state of Sr^{89} (Fig. 8), for which the expected shell-model configuration is $2d_{5/2}$. Considerable effort was expended without appreciable success in an attempt to fit the observed angular distribution on the basis of this assignment. The failure in this case may perhaps be the result of the relatively low energy resolution of the experiment, and the use of a naturally occurring isotopic mixture of elements for the target, making possible the existence of unresolved energy groups. In contrast, as has been mentioned, excellent results are obtained for the reaction leading to the 1.07-MeV level of Sr^{89} (Fig. 9).

Figures 10-16 present results of calculations for the ground state and 1.22-MeV level reactions of Zr^{90} for bombarding energies of 4, 10.85, and 13.6 MeV. Figure 10 for the 1.22-MeV first-excited state at a bombarding energy of 4 MeV (well below the Coulomb barrier) is interesting as an example of an $L_n=0$ reaction which does not have its principal peak at 0° . No measure-

⁹ F. B. Shull and A. J. Elwyn, Phys. Rev. **112**, 1667 (1959).

TABLE III. Elastic scattering parameters and related stripping parameters.^a

Target	Deuteron or proton ^b	Energy (MeV)	R_0 (F)	a (F)	V (MeV)	W (MeV)	Δ	σ_{th}/σ_{exp}	Figure	Reference
Co	<i>d</i>	4.07	1.50	0.682	52.9	17.4	0.022			c
Co ⁵⁹	<i>d'</i>	6.01	1.50	0.70	53	17		2.54	21	d
Cu	<i>p</i>	9.75	1.20	0.52	62	8.6				
Co ⁵⁹	<i>p'</i>	11.27	1.22	0.55	60	8.5				
Ni	<i>d</i>	13.5	1.43	0.63	59	19				e
Zn ⁶⁸	<i>d'</i>	11.9	1.43	0.63	59	19			22	
Cu	<i>p</i>	17.0	1.20	0.54	57.8	7.7	0.28			f
Zn ⁶⁸	<i>p'</i>	16.17	1.20	0.54	57.8	7.7				
Cu	<i>p</i>	17.0	1.29	0.51	47.6	7.6	0.22			f
Zn ⁶⁸	<i>p'</i>	16.17	1.29	0.51	47.6	7.6				
Cu	<i>p</i>	17.0	1.33	0.54	43.8	7.3	0.29			f
Zn ⁶⁸	<i>p'</i>	16.17	1.33	0.54	43.8	7.3				
Zn	<i>d</i>	11.8	1.40	0.594	71.2	27.7	0.108			g
Zn ⁶⁸	<i>d'</i>	11.9	1.40	0.594	71.2	27.7			23	
Zn	<i>d</i>	11.8	1.50	0.611	58.4	15.9	0.097			g
Zn ⁶⁸	<i>d'</i>	11.9	1.50	0.611	58.4	15.9				
Zn	<i>d</i>	11.8	1.60	0.599	50.6	12.5	0.141			g
Zn ⁶⁸	<i>d'</i>	11.9	1.60	0.599	50.6	12.5				
Cu	<i>p</i>	17.0	1.29	0.51	47.6	7.6	0.22			f
Zn ⁶⁸	<i>p'</i>	16.17	1.29	0.51	47.6	7.6				
Zr	<i>d</i>	11.8	1.49	0.802	55.6	19	0.13			g
Zr ⁹⁰	<i>d'</i>	10.85	1.49	0.75	55.6	14		3.18, 2.72	24, 25	
Zr	<i>p</i>	10.5	1.22	0.532	57.9	8.5	0.112			h
Zr ⁹⁰	<i>p'</i>	15.87	1.22	0.532	57.9	7				
Sn	<i>d</i>	15.0	1.60	0.58	55	11		2.03, 1.79	26, 27	e
Sn ¹¹⁶	<i>d'</i>	15.0	1.60	0.58	51	11				
Sn	<i>p</i>	19.6	1.20	0.445	54.8	10.2	0.198			i
Sn ¹¹⁶	<i>p'</i>	19.85	1.20	0.445	54.8	10.2				
Xe	<i>d</i>	10.95	1.55	0.597	44.7	10.1	0.168		19, 20	j
Ce ¹⁴⁰	<i>d'</i>	10.85	1.48	0.75	48	12				
Pb	<i>d</i>	15.0	1.52	0.63	48.5	9				e
Pb ²⁰⁶	<i>d'</i>	10.85	1.52	0.58	52	12		3.24	28	
Pb ²⁰⁸	<i>d'</i>	15.0	1.52	0.63	53.5	9		0.986	29	
Au	<i>p</i>	17.0	1.20	0.55	63.1	8.2	0.07			f
Pb ²⁰⁶	<i>p'</i>	15.36	1.20	0.55	63.1	9				
Pb ²⁰⁸	<i>p'</i>	14.71	1.20	0.55	63.1	8.2				

^a In the cases for which two figures (corresponding to different states) are listed the parameters used are the same for both reactions and the proton energy given corresponds to the ground-state reaction. Δ is the root-mean-square deviation of the theoretical points referred to the experimental points obtained in the manner described in reference 9.

^b The symbols *p* and *d* indicate that the subsequent parameters refer to the elastic scattering of protons and deuterons; similarly *p'* and *d'* designate the stripping proton and deuteron parameters.

^c I. Slaus and W. P. Alford, Phys. Rev. **114**, 1054 (1959).

^d A. E. Glassgold, W. B. Cheston, M. L. Stein, S. B. Schuldt, and G. W. Erickson, Phys. Rev. **106**, 1207 (1957).

^e See reference 8.

^f See reference 7.

^g G. Igo, W. Lorenz, and U. Schmidt-Rohr, Phys. Rev. **124**, 832 (1961).

^h L. Rosen, J. E. Brolley, and L. Stewart, Phys. Rev. **121**, 1423 (1961).

ⁱ R. A. Vanetsian, A. P. Klutcharov, and E. D. Fedtchenko, *Comptes Rendus du Congrès International de Physique Nucléaire; Interactions Nucléaires aux Basses Energies et Structure des Noyaux*, Paris, July, 1958 (Dunod, Paris, 1959), p. 607.

^j M. Takeda, J. Phys. Soc. Japan **15**, 557 (1960).

ments exist at this energy, and it would be interesting to see to what extent the calculated curve agrees with experiment. The results shown for the ground-, and first-excited levels at a bombarding energy of 10.85 MeV in Figs. 11 and 12, and for 13.6 MeV in Figs. 15 and 16 are in excellent accord with the observed angular distributions. The nuclear optical potentials for the two levels are seen to be nearly identical. The effect of varying the cutoff radius is illustrated in Figs. 13 and 14 for the same case as for Fig. 12. It is seen that the contribution to stripping arising from the interior of the nucleus is relatively unimportant for the angular distribution. On the other hand, varying the cutoff through the surface region of the nucleus is seen to have a considerable effect, especially on the diffraction minima, and on the back-angle distribution.

Angular distributions for reactions leading to the ground state and the 0.16-MeV level of the residual

nucleus Sn¹¹⁷ for a bombarding energy of 15 MeV are presented in Figs. 17 and 18. The agreement with experiment in the measured range is seen to be good, though it would be interesting to have data for angles greater than 70° to see to what extent the agreement persists for larger angles. Here, too, the nuclear optical potentials for the two levels are very nearly the same.

Finally, this first series of calculations concludes with the angular distributions for the reactions leading to the ground state and the 0.65-MeV level of Ce¹⁴¹ for a bombarding energy of 10.85 MeV (Figs. 19 and 20). The agreement again, in general, is good, particularly for the 0.65-MeV level reaction. It will be noted that the same optical parameters are used for the two states.

Results of calculations based on elastic scattering parameters are shown in Figs. 21–29. Except for Figs. 28 and 29 for the target nuclei Pb²⁰⁶ and Pb²⁰⁸, respec-

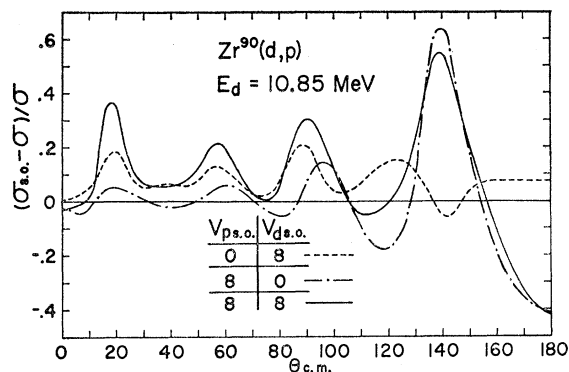


FIG. 30. Same case as Fig. 12, except that spin-orbit interactions in the deuteron and proton channels have been included.

tively, the angular distributions presented are for reactions previously mentioned. Table III lists the values of the nuclear parameters used. Except for the case of the reactions leading to the ground state of Co^{60} and to the ground state and the 0.16-MeV level of Sn^{117} (Figs. 21, 26, and 27), the elastic scattering parameters and those obtained on a trial-and-error basis are quite similar, as are the corresponding angular distributions. It must again be emphasized, however, that there is always a certain ambiguity in the values of the optical parameters so determined.

It is a well-known result from optical model studies of elastic scattering data that similar angular distributions can be obtained for a range of radii if the other parameters, especially the real potential, are suitably adjusted.⁹ The corresponding behavior for stripping has been investigated for Zn^{68} using best-fit elastic scattering parameters for several different radii for proton and deuteron interactions. The results are shown in Figs. 22 and 23. It will be noted that the curves differ appreciably from each other, especially those in Fig. 23 for which the deuteron radius is varied. Consequently, it appears advisable in using elastic scattering parameters for stripping to vary the radius in the hopes of improving the fit. Indeed, the best result for Zn^{68} is obtained using a deuteron radius of 1.4 F, and there is some indication that the deuteron radius for stripping for other reactions might more properly lie from 1.3 to 1.4 F, rather than in the range 1.5 to 1.6 F found from elastic scattering studies.⁸ A more detailed investigation of this matter is being carried out.

The ratios of the theoretical to experimental absolute cross sections, calculated at the principal peak, are listed in Tables II and III for those cases for which experimental absolute cross sections are available. Generally, the values lie in the range 2 to 3. This would seem to indicate that the residual nucleus spends only one-half to one-third of its time in the configuration "inert core+neutron." These numbers, of course, are dependent on the parameters used. However, the fact that the ratios for stripping to different levels in Zr^{91}

and in Sn^{117} show fairly good agreement with each other indicates that they may be meaningful. In addition, for stripping from Pb^{208} the ratio is nearly one, as might be expected, since the doubly closed shells of Pb^{208} should form a particularly inert core.

SPIN-ORBIT RESULTS

The effect of spin-orbit interactions¹⁰ on the $\text{Zr}^{90}(d,p)\text{Zr}^{91}$ 1.22-MeV level angular distribution is shown in Fig. 30. The polarization for the same reaction also has been computed, and is plotted in Fig. 31. Actually, spin-orbit calculations have been made for all the stripping reactions discussed previously for which the total neutron angular momentum quantum number is $1/2$. In no case has it been found for $A \geq 68$ that inclusion of the spin-orbit terms improves the angular distribution. In general, the spin-orbit interaction smooths out the angular distribution without affecting the position of the principal peak. The spin-orbit effect is particularly large at the backward angles, for which accurate measurements, unfortunately, are lacking.

Experimental polarization data for an $L_n=0$ reaction for medium or heavy weight targets, similar to those of Isoya¹¹ and Evans¹² for light targets, would be particularly helpful in evaluating the role of spin-orbit interactions in nuclear reactions, since for this case zero polarization is predicted in the absence of such interactions. The polarization curve shown in Fig. 31 is included as an example of the results to be expected from the optical model.

It is to be noted in Figs. 30 and 31 that the angular distribution for the proton and deuteron spin-orbit interactions taken together is roughly the sum of the

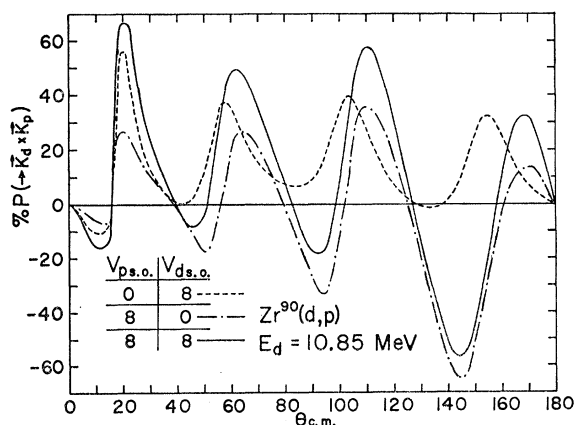


FIG. 31. Polarization of the outgoing proton with inclusion of spin-orbit interactions for the case given in Fig. 12.

¹⁰ D. Robson, *Nuclear Phys.* **22**, 34 (1961).

¹¹ A. Isoya, S. Micheletti, M. J. Marrone, and L. H. Reber, *Proceedings of the Rutherford Jubilee International Conference, Manchester, 1961* (Heywood and Company Ltd., London, 1961), p. 595.

¹² J. E. Evans, J. A. Kuehner, and E. Almqvist, *Bull. Am. Phys. Soc.* **7**, 60 (1962).

distributions of the interactions taken separately. This result has been predicted by Newns,¹³ assuming that the spin-orbit interaction is a small perturbation. Figures. 30 and 31 also illustrate the general result previously noted that any structural feature (i.e., the curve or its first or second derivative) of either the polarization or the angular distribution can usually be correlated with a structural feature of the other.

DISCUSSION

The results presented here are for nuclei with $A \geq 59$, although calculations have been made for lighter nuclei, and it is hoped to discuss these in detail at a later time. With some exceptions, the calculations for nuclei with $A < 30$ have not given very satisfying results. Experimental cross sections beyond the first peak are often larger than the calculated cross sections, some of the parameters exhibit a large variation with changes in bombarding energy, there may be little parameter consistency between reactions leading to different levels of the same nucleus, and elastic scattering parameters are found to yield inferior results when applied to stripping.

In general, then, the optical model results that have been obtained for the medium and heavy nuclei are distinctly better than those for the lighter nuclei. There are several possible explanations for this. For the heavier nuclei center-of-mass corrections become more accurate, the point-mass and the zero-range neutron-proton potential approximations for the deuteron are better for larger targets, the use of the optical model is more reasonable, exchange stripping is expected to be generally small, and compound nucleus effects should be relatively smaller because of the higher level density found in heavier nuclei.

The results obtained here confirm the validity of the distorted wave Born approximation, as well as that of the optical model, for targets with $A \geq 59$. The fact that stripping angular distributions for different levels

of the residual nucleus can be reproduced using the same interaction potentials suggests that the basic stripping theory is essentially correct. Similarly, the use of the optical model seems justified by the present results in the sense that the expected parameter consistency between different nuclei for stripping, as well as between stripping and elastic scattering parameters, is obtained to a fair degree in most cases.

Stripping on light elements has been used extensively as a spectroscopic tool to determine the properties of nuclear energy levels. Similar work on heavier elements has been more limited for various reasons. The energy levels are more closely spaced and, therefore, harder to resolve, the lighter elements have been of greater theoretical interest, and many institutions do not have accelerators of sufficient energy to make stripping results on heavy targets interpretable by the simple Butler theory.

The authors suggest here a possible solution to the latter difficulty. We have written, and propose to make available to interested persons, a distorted wave (d, p) and (d, n) stripping reaction program for $L_c \leq 6$ in the widely used FORTRAN programming language, which should be readily adaptable to any computer accepting this language and having a storage capacity of 8000 words or more. Its assembly time is approximately 2 min, and the average running time for a given case is about 45 sec.⁴ The program, its description, and instructions for its use will be provided on request. The results of this article can be used as a guide in determining values of the optical-model parameters necessary for the calculations.

ACKNOWLEDGMENTS

We are indebted to Dr. John L. Richter for his help with the preliminary stages of this work, and to Henry Stoppelbein of the University of Texas Computation Center for his assistance in running the programs. It is also a pleasure to acknowledge helpful discussions with Dr. B. B. Kinsey, Dr. H. C. Newns, Dr. W. Tobocman, and Dr. L. Stewart.

¹³H. C. Newns and M. Y. Refai, Proc. Phys. Soc. (London) **A71**, 627 (1958).